

# Gyrostat Trajectories and Core Energy

M. Guelman\*

*International Telecommunications Satellite Organization, Washington, D.C.*

A geometric study is performed of the angular momentum trajectories for platform axes of an asymmetric and dynamically unbalanced gyrostat with a constant rotor/platform relative rate. A new relation is established between these trajectories and the core energy. Based on this relation, the effects of energy dissipation, both in the rotor and platform, on the gyrostat stability is analyzed.

## Introduction

**T**ORQUE-free, rigid-body gyrostat dynamic behavior has been rigorously studied in the past in analytical terms<sup>1,2</sup> and by qualitative methods.<sup>3</sup> Actual spacecraft of the gyrostat type contain flexible parts, dampers, and fuel slosh, all of which are sources of energy dissipation and that sensibly modify the system's dynamic behavior.

The analysis and simulation of dissipative spacecraft is so difficult that workers in this field have often resorted to heuristic methods in order to be able to design such systems. One such method is the so-called energy-sink approach, widely employed for the analysis and design of dual spin spacecraft.<sup>4-6</sup>

Even though the use of this technique in many cases provided the right answers for a successful spacecraft design, it was accompanied by strong disclaimers and even counterexamples,<sup>7</sup> in particular for the case of systems containing driven rotors. The main contention has been that the presence of driven rotors necessarily implies energy sources, contradicting the basic assumption that in the presence of passive dissipation devices the rotational kinetic energy is a decreasing function of time.

In Ref. 7 a new hypothesis was advanced, and further studied in Ref. 8, that for a system containing a driven rotor and a dissipative device in the platform, the rotational kinetic energy, less that due to the rotor rotation, relative to the platform itself (a so-called "core" energy) is effectively a decreasing function of time.

The purposes of this work are 1) to perform an analytic-geometric study of the attitude motion of a gyrostat with an asymmetric unbalanced platform and symmetric balanced rotor with a constant rotor/platform relative rate, 2) to establish a relation between the system attitude integral curves and the gyrostat "core" energy, and 3) to determine the system behavior under energy dissipation.

## The System Model

In Fig. 1 a gyrostat is depicted with a balanced and symmetric rotating rotor and an asymmetric and dynamically unbalanced platform.

The platform and rotor tensors of inertia in their own fixed coordinates, referring to the spacecraft center of mass, are respectively defined by

$$[I_P] = \begin{bmatrix} I_1^P & 0 & -I_{13}^P \\ 0 & I_2^P & 0 \\ -I_{13}^P & 0 & I_3^P \end{bmatrix} \quad (1)$$

$$[I_R] = \begin{bmatrix} I_T^R & 0 & 0 \\ 0 & I_T^R & 0 \\ 0 & 0 & I_3^R \end{bmatrix} \quad (2)$$

The column matrix of components of the total spacecraft angular momentum decomposed along the platform axes is given by

$$h = I w_p + h_r \quad (3)$$

where  $w_p$  is the column matrix of the three components of angular velocity of the platform resolved along the platform,  $I$  is the gyrostat tensor of inertia in platform fixed coordinates, defined by

$$I = I_P + I_R = \begin{bmatrix} I_1 & 0 & -I_{13} \\ 0 & I_2 & 0 \\ -I_{13} & 0 & I_3 \end{bmatrix} \quad (4)$$

and  $h_r$  is defined by

$$h_r = I_R w_r = (0, 0, h_r)^T \quad (5)$$

where  $w_r = (0, 0, w_r)^T$  is the rotor to platform relative angular rate,  $h_r = I_3^R w_r$  and  $T$  denotes the transpose matrix.

The system equations of motion with no external torques are defined by

$$\dot{h} + (w_p \times h) = 0 \quad (6)$$

where  $w_p \times$  is the matrix that stands for the vector product operation, i.e.,

$$w_p \times = \begin{bmatrix} 0 & -w_{p3} & w_{p2} \\ w_{p3} & 0 & -w_{p1} \\ -w_{p2} & w_{p1} & 0 \end{bmatrix} \quad (7)$$

with the dot denoting the component-wise time derivative  $d/dt$ . Substituting  $w_p$  from Eq. (3) into Eq. (6)

$$\dot{h} + [I]^{-1}(h - h_r) \times h = 0 \quad (8)$$

Development of Eq. (8) gives

$$\dot{h}_1 = (a_3 - a_2)h_2h_3 - a_3h_rh_2 + ch_1h_2 \quad (9)$$

$$\dot{h}_2 = (a_1 - a_3)h_1h_3 + a_3h_rh_1 - c(h_1^2 - h_3^2 + h_rh_3) \quad (10)$$

$$\dot{h}_3 = (a_2 - a_1)h_1h_2 - ch_2(h_3 - h_r) \quad (11)$$

Received Aug. 28, 1986; revision received July 10, 1987. Copyright © American Institute of Aeronautics and Astronautics, Inc., 1987. All rights reserved.

\*Control Engineer; currently at Ministry of Defence, Rafael, Israel.

where  $h_1, h_2, h_3$  are the components of  $\mathbf{h}$  in platform coordinates and  $a_1, a_2, a_3$  are the components of the  $[I]^{-1}$  matrix,

$$[I]^{-1} = \begin{bmatrix} a_1 & 0 & c \\ 0 & a_2 & 0 \\ c & 0 & a_3 \end{bmatrix} \quad (12)$$

with

$$a_1 = I_3/(I_1 I_3 - I_{13}^2) \quad (13)$$

$$a_2 = 1/I_2 \quad (14)$$

$$a_3 = I_1/(I_1 I_3 - I_{13}^2) \quad (15)$$

$$c = I_{13}/(I_1 I_3 - I_{13}^2) \quad (16)$$

Eqs. (9–11) define the dynamic behavior of the gyrostat.

### The Analytic Solution

Even though this system is highly nonlinear, a closed-form solution can be obtained for the case of a constant rotor to platform relative rate, as will now be shown.

Since there are no external torques

$$h_1^2 + h_2^2 + h_3^2 = h^2 \quad (17)$$

Now, since  $\mathbf{w}_p$  is normal to  $\mathbf{w}_p \times \mathbf{h}$  it follows from Eq. (6)

$$\mathbf{w}_p^T \dot{\mathbf{h}} = 0 \quad (18)$$

Substituting  $\mathbf{w}_p$  from Eq. (3) into Eq. (18)

$$\{[I]^{-1}(\mathbf{h} - \mathbf{h}_r)\}^T \dot{\mathbf{h}} = 0 \quad (19)$$

For a constant rotor to platform relative rate

$$\dot{\mathbf{h}} = \dot{\mathbf{h}} - \dot{\mathbf{h}}_r \quad (20)$$

Substituting Eq. (20) into Eq. (19) and rearranging

$$(\dot{\mathbf{h}} - \dot{\mathbf{h}}_r)^T [I]^{-1}(\mathbf{h} - \mathbf{h}_r) = 0 \quad (21)$$

It follows that

$$(\mathbf{h} - \mathbf{h}_r)^T [I]^{-1}(\mathbf{h} - \mathbf{h}_r) = \text{const} \quad (22)$$

Development of Eq. (22) in terms of its components and taking into account the relation (17) gives

$$(a_1 - a_2)h_1^2 + (a_3 - a_2)h_3^2 + 2ch_3h_1 - 2ch_rh_1 - 2a_3h_rh_3 = k \quad (23)$$

where  $k$  is defined by the initial conditions.

This integral is a conic, whose indicator is defined by

$$i = (a_2 - a_1)(a_3 - a_2) + c^2 \quad (24)$$

The sign of the indicator will define whether this conic is a hyperbola or an ellipse.

In terms of the system moments of inertia, assuming  $I_{13}^2 < I_1 I_3$  (which is normally the case), the indicator  $i$  is positive for

$$I_{13} < I_3^P < I_2 < I_1^* \quad (25)$$

where

$$I_1^* = [(I_1 + I_3^P)/2] + [(I_1 - I_3^P)^2/4 + I_{13}^2]^{1/2} \quad (26)$$

For a positive  $i$  the integral is a hyperbola in the  $h_1, h_3$  plane.

For

$$I_{13} < I_3^P < I_1^* < I_2 \quad (27)$$

$i$  is negative, implying that the integral is an ellipse. The limiting case  $I_2 = I_1^*$  corresponds to two straight lines.

The system integral curves are then defined by the intersection of the conic cylinder, defined by Eq. (23) (with a hyperbolic or elliptic cross section, depending on the values of the moments of inertia) with the sphere defined by Eq. (17). These integral curves in the  $h_1, h_2, h_3$  space are symmetric with respect to the  $h_1, h_3$  plane.

### The Geometric Analysis

The analytic solution obtained in the previous section enables us to study particular trajectories of the system. However, these trajectories do not provide a general picture of the system behavior over the entire state space. For this purpose, use will now be made of geometric methods. The use of these methods, together with the integral curves previously obtained, will provide the general picture of the system behavior.

In order to perform the geometric analysis, the equilibrium points of the system will have to be first determined.

The equilibrium points are determined by the following three equations, corresponding to the null values of  $\dot{h}_1, \dot{h}_2, \dot{h}_3$ ,

$$h_2[(a_3 - a_2)h_3 + ch_1 - a_3h_r] = 0 \quad (28)$$

$$ch_1^2 - ch_3^2 - (a_1 - a_3)h_1h_3 - a_3h_rh_1 + ch_rh_3 = 0 \quad (29)$$

$$h_2[(a_2 - a_1)h_1 - ch_3 + ch_r] = 0 \quad (30)$$

together with Eq. (17).

The behavior of these equations will now be studied in the  $h_1, h_3$  plane.

The intersection of the  $h_1, h_3$  plane and the sphere  $S$ , defined by Eq. (17), defines a circle  $C$  of radius  $h$ , centered at the origin. This circle delimits in the  $h_1, h_3$  plane the existence region of the system solutions.

Eqs. (28–30) define three different surfaces in the state space, and the intersections of these surfaces with the  $h_1, h_3$  plane will now be considered.

In the  $h_1, h_3$  plane, the locus of points satisfying Eq. (28) is the circle  $C$  and the straight line

$$(a_3 - a_2)h_3 + ch_1 - a_3h_r = 0 \quad (31)$$

The locus of points defined by Eq. (29) is a hyperbola crossing the  $h_3$  axis at  $h_r$  and the origin, and the  $h_1$  axis at  $h_1 = a_3h_r/c$ .

The locus of points satisfying Eq. (30) is the circle  $C$  and the straight line.

$$(a_2 - a_1)h_1 - ch_3 + ch_r = 0 \quad (32)$$

All these different loci are depicted in Fig. 2. The common intersections of the three previous loci fulfill simultaneously Eqs. (28–30) and consequently define the equilibrium points of the system, provided they are inside the circle of existence  $C$ .

As can be seen, from the example considered in Fig. 2, there are six valid equilibrium points. Four of these points are the result of the intersection of the hyperbola and the circle  $C$ . The triple intersection of the two straight lines and the hyperbola corresponds to a double equilibrium point on the sphere  $S$ , for positive and negative  $h_2$ , respectively. This intersection has coordinates  $h_1 = ca_2h_r/i$ ,  $h_3 = [a_3(a_2 - a_1) + c^2]h_r/i$ , with  $i$  as defined in Eq. (24).

It can readily be shown, by simple algebraic manipulations, that the equilibrium points belonging to the circle  $C$  correspond to the cases where the complete integral (the conic cylinder) obtained in the previous section is tangent to the sphere  $S$ .

As already indicated,  $h_r$  is the system parameter. As seen in Fig. 2, increasing or decreasing the value of  $h_r$  will shift the hyperbola as well as the two straight lines, upwards or downwards, respectively. This modifies the position of the equilibrium points and, even more fundamentally their number. Varying  $h_r$ , the system will have at the most six equilibrium points and at the least two equilibrium points.

For example, for  $h_r = h$  (the entire system momentum is in the rotor) the system has only two equilibrium points, one just at the top of the circle  $C$  and the other close to its bottom.

Now, depending on the values of the moments of inertia, the triple crossing point can be on the left or right  $h_1, h_3$  half plane. This depends on the same constant  $i$  that defined the integral conic type.

For positive  $i$  the intersection is in the right half plane, and for negative  $i$  in the left half plane. For  $i = 0$ , the two straight lines defined by Eqs. (31) and (32) are parallel. As before, the sign of  $i$  is determined by the relative values of the moments of inertia.

The system integral curves will now be presented as functions of the system parameters,  $h_r$  and the system moments of inertia.

Figs. 3 and 4 show, for different values of  $h_r$ , the two cases of a prolate and oblate spacecraft. Depending on the value of  $h_r$ , both positive and negative, the system has, as was already shown, a maximum of six equilibrium points and a minimum of two. In the case of six equilibrium points, those on the circle  $C$ , four in number, are centers and the two internal points to  $C$  (corresponding to positive and negative  $h_2$ ) are saddle points. For the case of two equilibrium points, both of them are centers.

### Core Energy

It is our purpose now to establish a relation between the system integral curves and the gyrostat energy.

For the free-torque case it can be shown that the kinetic energy is a complete integral of the free-torque gyrostat equations of motion,<sup>1</sup> or, in other terms, the gyrostat integral curves are lines of constant kinetic energy.

For the case here studied, torque is to be applied to maintain a constant relative rate. It should be expected, then, that the gyrostat integral curves are no longer lines of constant kinetic energy.

What is, then, the relation between the system energy and its integral curves?

In order to provide an answer, the concept of core energy, as proposed in Ref. 8 and further developed in Ref. 9, will now be reviewed.

The core energy is defined as being equal to the total kinetic energy of the spacecraft minus that portion of the rotor energy that is due to the relative rotation between the rotor and the platform. The main idea behind this definition is to obtain a positive definite function, eliminate the effects of energy sources, and be able to apply energy-sink concepts. Clearly, if the nutation angle undergoes a change, the gyrostat total angular momentum component along the spin axis also changes. Since, in the absence of an applied torque, and independently of the nutation angle, the absolute angular rate of the symmetric, balanced rotor along the spin axis is a constant, energy must either be put into or removed from the system in order to maintain the rotor at a constant relative speed. The core energy puts aside this energy term.

The energy due to motion of the rotor relative to the platform is defined in Ref. 8 as

$$E_m = 1/2 \cdot I_3^R (\omega_P + \omega_r)^T (\omega_P + \omega_r) - 1/2 \cdot I_3^R \omega_P^T \omega_P \quad (33)$$

It is worthwhile to note the relation of this energy term to the power expended, or absorbed, to keep  $\omega_r$  constant.<sup>9</sup> This electromechanical power  $P_m$  is defined by

$$P_m = T \omega_r \quad (34)$$

where  $T$  is the torque required to maintain a constant relative rate. This torque  $T$  is defined by the rotor moment equation and for the case of a constant relative rate is given by

$$T = I_3^R \dot{\omega}_{P3} \quad (35)$$

where  $\dot{\omega}_{P3}$  is the platform angular acceleration component along the spin axis.

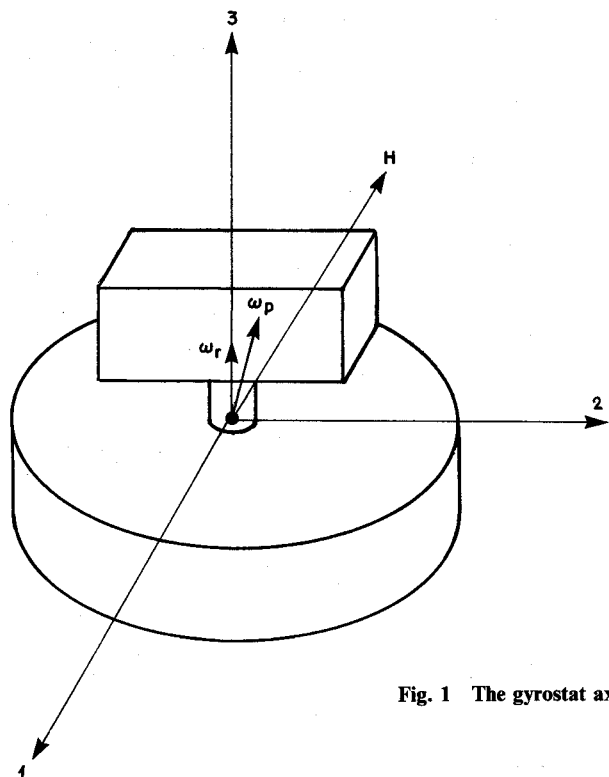


Fig. 1 The gyrostat axes.

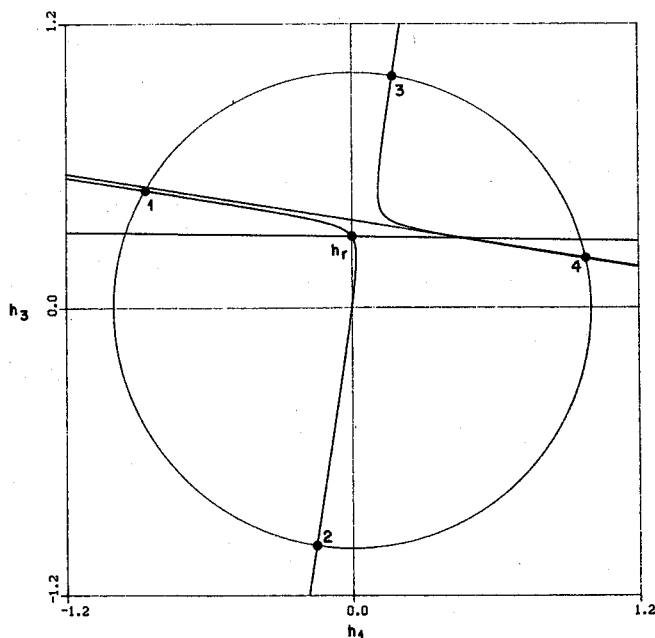


Fig. 2. The equilibrium points.

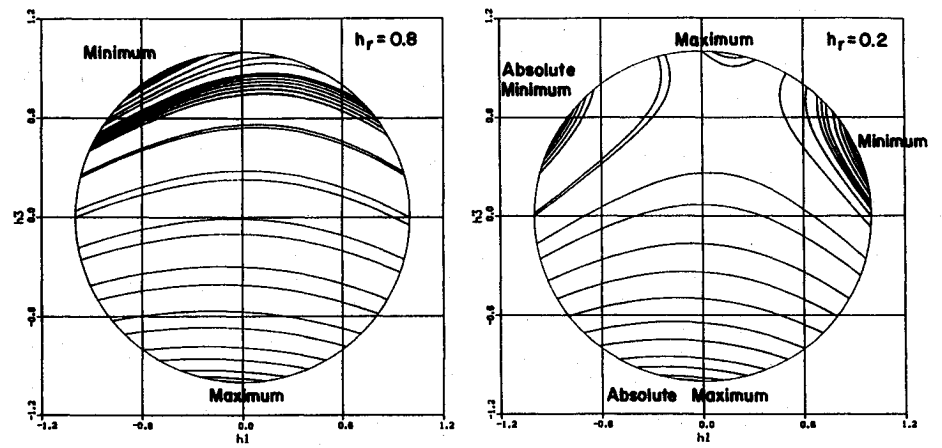


Fig. 3. Prolate gyrostat integral curves.

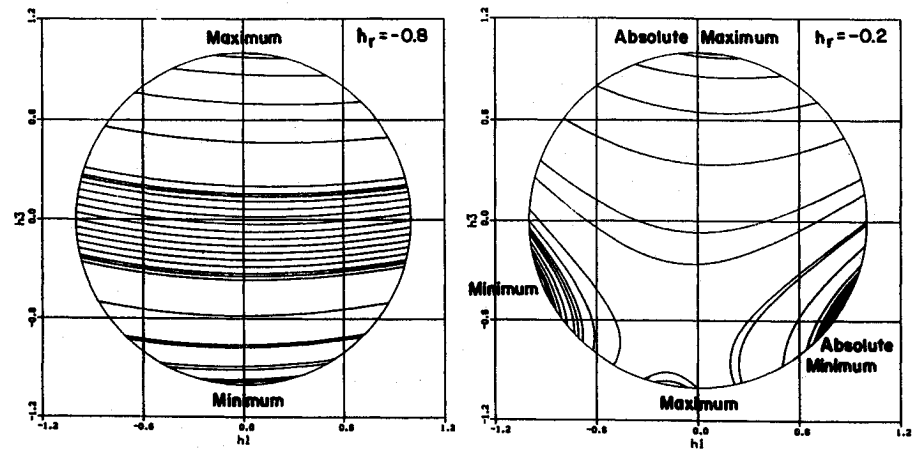
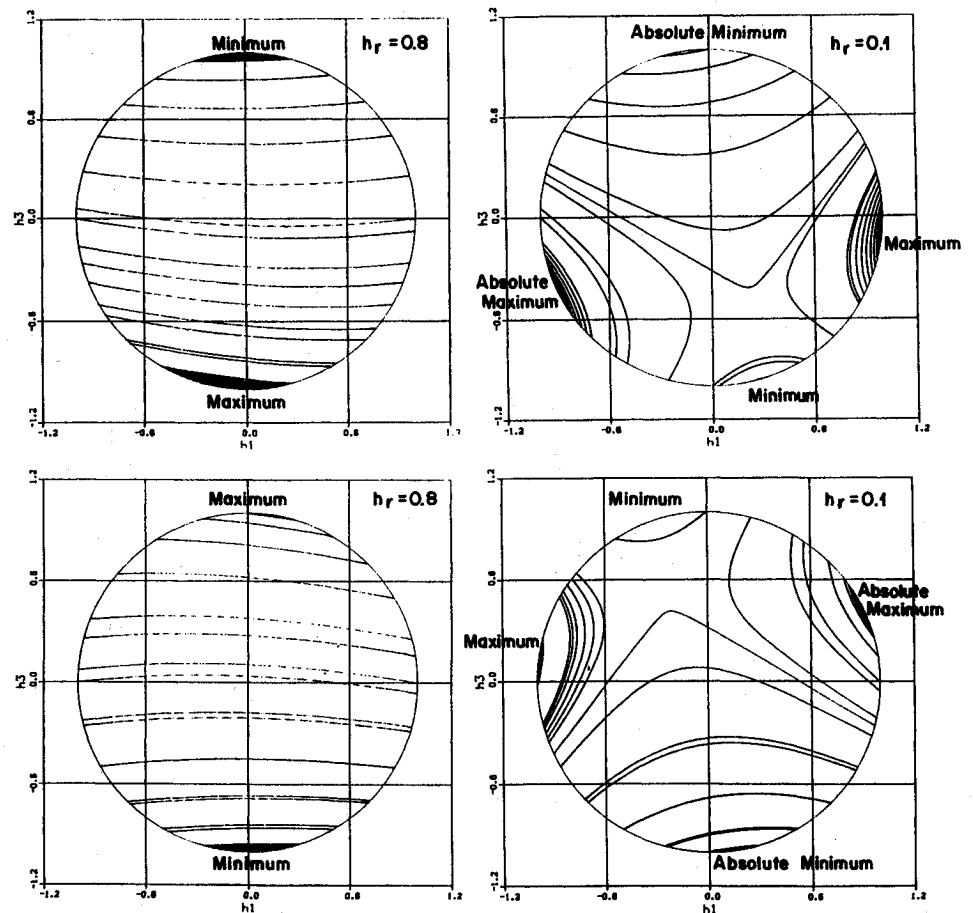


Fig. 4. Oblate gyrostat integral curves.



It follows, then, that

$$P_m = h_r \dot{w}_{P3} \quad (36)$$

Differentiating  $E_m$  with respect to time,

$$E_m = h_r \dot{w}_{P3} = P_m \quad (37)$$

is obtained.

The spacecraft kinetic energy is defined by

$$E = 1/2 \cdot w_p^T [I_p] w_p + 1/2 \cdot w_R^T [I_R] w_R \quad (38)$$

where

$$w_R = w_p + w_r \quad (39)$$

is the column matrix of the three components of the rotor absolute angular rate.

The gyrostat core energy is defined by

$$E_c = E - E_m \quad (40)$$

Introducing  $E$  and  $E_m$  from Eqs. (38) and (33), respectively, into Eq. 40, and rearranging, results in

$$E_c = 1/2 \cdot w_p^T [I] w_p \quad (41)$$

Introducing  $w_p$  from Eq. (3) into Eq. (41) and taking into account Eq. (22) results in

$$E_c = 1/2(h - h_r)^T [I]^{-1} (h - h_r) = \text{const} \quad (42)$$

The core energy is a constant along the gyrostat system integral curves for a constant platform/rotor rate.

Because the system integral curves are lines of constant core energy, the extrema of core energy will also be the equilibrium points of the system, as will now be shown. The extrema core energy states are the solutions<sup>10</sup> of

$$\partial G / \partial h_i = 0, i = 1, 2, 3 \quad (43)$$

together with Eq. (17), where

$$G = E_c + p(h^2 - h_1^2 - h_2^2 - h_3^2) \quad (44)$$

and  $p$  is a Lagrange multiplier.

The solutions of this system satisfy

$$h_1^2 + h_3^2 = 0 \quad (45)$$

$$ch_1^2 - ch_3^2 + (a_3 - a_1)h_1h_3 + ch_1h_3 - a_3h_1h_1 = 0 \quad (46)$$

These are precisely the same conditions defining the equilibrium points on the circle  $C$ : These equilibrium points are the extrema of the system core energy.

A map of core energy can be now obtained by simply labeling the system integral curves with their constant respective values. The results for the cases of a prolate and oblate spacecraft are presented in Figs. 3 and 4, respectively.

### Platform Energy Dissipation

Core energy maps will now be used to study the gyrostat behavior under passive energy dissipation.

In Refs. 8 and 9 it was shown that the following basic assumption holds true: For an energy dissipating device in the platform, the core energy is a decreasing function of time.

Under this assumption, and according to the core maps presented in Figs. 3 and 4, the following results can be stated.

### Case A: $I_3 < I_2 < I_1$ , prolate gyrostat

For  $h_r > h_l$  the system has one globally stable equilibrium point corresponding to  $h_3 > 0$ .

From two to a higher number of equilibrium points,  $h_l$  is the transition value of  $h_r$ , as shown in Fig. 5a (see also Fig. 3).

For  $|h_r| < h_l$ , the system has two stable equilibrium points, for  $h_1$  positive and negative, respectively.

For  $h_r < -h_l$  the system has one globally stable equilibrium point with  $h_3 < 0$ . The gyrostat acquires, at the equilibrium state, an upside-down attitude.

### Case B: $I_3 > I_2 > I_1$ , oblate gyrostat

For  $h_r > h_l$  the system has one globally stable equilibrium point corresponding to  $h_3 > 0$ . Note that  $h_l$  is shown in Fig. 5b (see also Fig. 4).

For  $|h_r| < h_l$ , the system has two stable equilibrium points, for  $h_3$  positive (upright attitude) and negative (downright attitude), respectively.

For  $h_r < -h_l$ , the system has one globally stable equilibrium point with  $h_3 < 0$ . The gyrostat acquires at the equilibrium state an upside-down attitude.

For  $h_r = 0$ , the single spinner cases, the electromechanical energy is null and the core and kinetic energy coincide. This is clearly the only case where this occurs. In general, depending on the value of  $h_r$ , the kinetic energy can decrease or increase for a decreasing core energy. This was already pointed out in Ref. 9.

### Rotor Energy Dissipation

In all the previous works already mentioned, only the case of energy dissipation in the platform was considered, although it is clear that energy dissipation can be present in the rotor as well. This is the case when, for instance, the presence of liquid fuel sloshing in the rotor becomes the dominant energy dissipation mechanism.

Since from a mathematical viewpoint nothing apparently differentiates the platform from the rotor, an entirely symmetric analysis could, in principle, be utilized for studying the effects of energy dissipation in the rotor. However, careful attention is to be paid to the fact that in this study the rotor was assumed symmetric and balanced, as opposed to an asymmetric, unbalanced platform. The rotor tensor of inertia components has the same values, both in rotor and platform coordinates. This is not the case for the platform tensor of inertia components.

Let us now derive for the rotor the expression for the core energy.

The electromechanical energy as seen now from the rotor can be defined as

$$E_m^R = 1/2 \cdot (w_R - w_r)^T [I_p] (w_R - w_r) - 1/2 \cdot w_R^T I_F w_R \quad (47)$$

The corresponding core energy as seen from the rotor is defined by

$$E_c^R = E - E_m^R \quad (48)$$

Now, even though the value of the electromechanical energy as defined in Eq. (47) is independent of the system of coordinates, the computation itself heavily depends on the choice of coordinate system. Because the computation of each term should be carried out with all the components defined in a single system of coordinates, the expression of  $E_m^R$  can be most easily obtained in platform coordinates and the following equivalent form is to be employed:

$$E_m^R = 1/2 \cdot w_p^T [I_p] w_p - 1/2 \cdot (w_p + w_r)^T [I_p] (w_p + w_r) \quad (49)$$

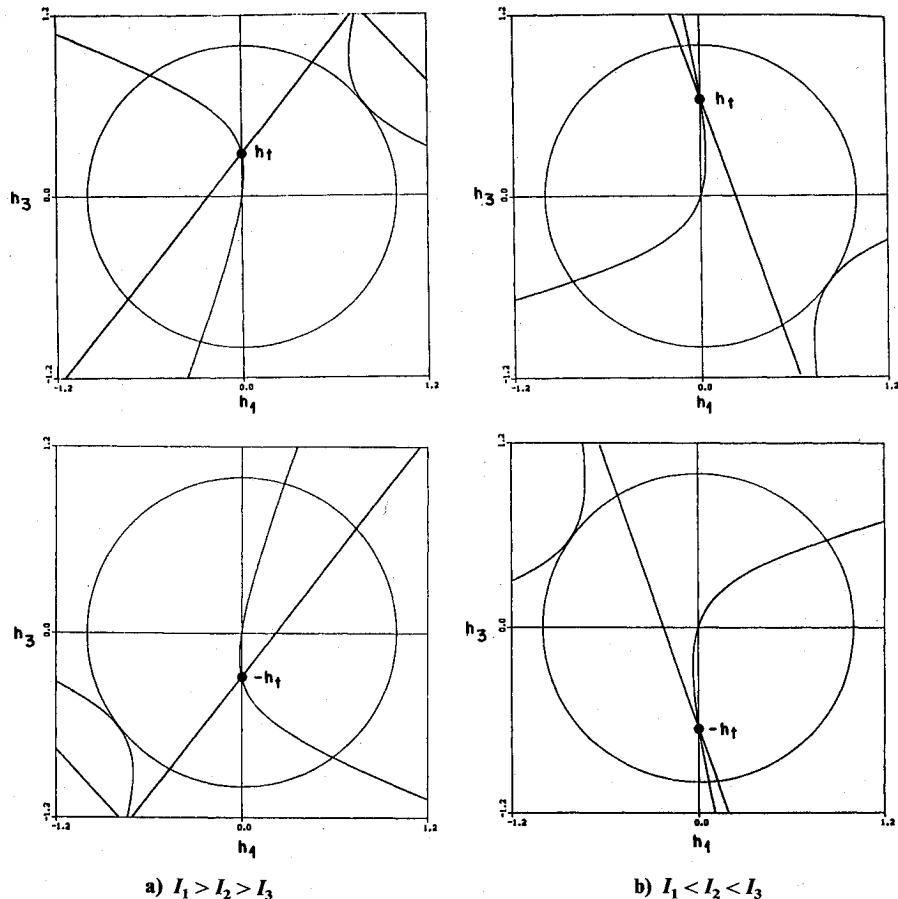


Fig. 5. The transition points.

Taking  $E$  from Eq. (33) and  $E_m^R$  from Eq. (49), rearranging, and taking into account Eq. (32), it is found that

$$E_c^R = 1/2 \cdot (w_p + w_r)^T [I] (w_p + w_r) \quad (50)$$

Operating, rearranging, and taking into account Eq. 41

$$E_c^R = E_c + w_p^T [I] w_r + 1/2 \cdot w_r^T [I] w_r \quad (51)$$

From the  $E_c^R$  expression it can be readily seen that the core energy, as seen from the rotor, is not constant along the gyrostat integral curves.

It is now worthwhile to find under what conditions the core energy, as seen from the rotor, is constant along the system integral curves. For this purpose  $E_c^R$  is evaluated in rotor coordinates. After some lengthy algebraic operations we find that

$$E_c^R = w_R^T [w_r \times ([B] I_P [B]^T w_R)] \quad (52)$$

where  $[B]$  is defined by

$$[B] = \begin{bmatrix} \cos(\Phi_r) & \sin(\Phi_r) & 0 \\ -\sin(\Phi_r) & \cos(\Phi_r) & 0 \\ 0 & 0 & 1 \end{bmatrix} \quad (53)$$

with  $\Phi_r$  the relative rotor to platform angle.

The core energy derivative along the system trajectories becomes identically zero for two particular cases: 1) where  $w_r = 0$ , i.e., the single spinner, and 2) where the platform is balanced and symmetric.

It should be remarked that the constancy of the core energy along the system trajectories, as seen from the rotor, for a symmetric and balanced platform, holds independently of the rotor inertia tensor; this can be seen from Eq. (52). It can,

therefore, be stated in a general form, that the relation existing between core energy and the system integral curves will hold whenever either one of the dual spinner parts is symmetric and balanced.

For the particular case of a symmetric and balanced rotor and platform, the expression for  $E_c^R$  becomes

$$E_c^R = (a_3 - a_2) h_3^2 / 2 + a_3 h_p h_3 \quad (54)$$

where

$$h_p = I_3^p w_r \quad (55)$$

In this case, it can be readily shown that the equilibrium point  $h_1 = h_2 = 0, h_3 = h$  (the upright attitude) is stable, under energy dissipation in the rotor if

$$(a_3 - a_2)h + a_3 h_p < 0 \quad (56)$$

After rewriting this inequality in terms of the rotor and platform absolute rates and rearranging, the result is

$$(I_3^R + I_3^p w_{F3} / w_R) / I_1 > 1 \quad (57)$$

where  $w_R$  is the rotor absolute rate along the spin axis.

This is precisely the same well-known result of the rotor effective inertia ratio.<sup>5</sup>

For the general case of both rotor and platform, asymmetric and unbalanced, the use of the core energy concept to prove system stability under energy dissipation is still open to further research.

### Summary

In this work a study of the behavior of an asymmetric and dynamically unbalanced gyrostat for a constant rotor to platform relative rate. A parametric closed-form solution was ob-

tained for the system integral curves and a geometric analysis was performed of the system behavior. A relation was established between the system integral curves and the core energy. This relation was shown to exist whenever either one of the dual spinner parts is symmetric and balanced. Based on this relation, the system behavior under energy dissipation, either in the rotor or platform, was studied and results were presented.

### Acknowledgments

The author wishes to thank L. Virdee and Drs. G. Gordon and V. Slabinski for their constructive comments. The author is also grateful to the reviewer for his helpful suggestions.

### References

<sup>1</sup>Leimanis, E., *The General Problem of the Motion of Coupled Rigid Bodies about a Fixed Point*, Springer-Verlag, New York, 1965, pp. 215-238.

<sup>2</sup>Cochran, J. E. Jr. and Shu, P. H., "Attitude Motion of Spacecraft with Skewed Internal Angular Momenta," *The Journal of the Astronautical Sciences*, Vol. XXXI, April-June 1983, pp. 203-215.

<sup>3</sup>Velman, J. R. and Belardi, J. W., "Gyrostat Attitude Dynamics," Hughes Aircraft Co., El Segundo, CA, Rept. SSD. 90154 R, May 1969.

<sup>4</sup>Likins, P. W., "Attitude Stability Criteria for Dual Spin Spacecraft," *Journal of Spacecraft and Rockets*, Vol. 4, Dec. 1967, pp. 1638-1643.

<sup>5</sup>Iorillo, A. J., "Hughes Gyrostat System," *Proceedings of the Symposium on Attitude Stabilization and Control of Dual Spin Spacecraft*, Hughes Aircraft Co., El Segundo, CA, Aug. 1967, pp. 257-266.

<sup>6</sup>Spencer, T. M., "Energy Sink Analysis for Asymmetric Dual Spin Spacecraft," *Journal of Spacecraft and Rockets*, Vol. 11, July 1974, pp. 463-468.

<sup>7</sup>Kane, T. A. and Levinson, D. A., "Energy Sink Analysis of Systems Containing Driven Rotors," *Journal of Guidance and Control*, Vol. 3, May-June 1980, pp. 234-238.

<sup>8</sup>Hubert, C., "Spacecraft Attitude Acquisition from an Arbitrary Spinning or Tumbling State," *Journal of Guidance and Control*, Vol. 4, March-April 1981, pp. 164-170.

<sup>9</sup>Cochran, J. E. Jr. and Shu, P. H., "Effects of Energy Addition and Dissipation of Dual Spin Spacecraft Attitude Motion," *Journal of Guidance and Control*, Vol. 6, Sept.-Oct. 1983, pp. 368-373.

<sup>10</sup>Athans, M. and Falb, P. L., *Optimal Control*, McGraw-Hill, New York, 1966, Section 5-4, pp. 233-236.

## Recommended Reading from the AIAA Progress in Astronautics and Aeronautics Series . . .



### Thrust and Drag: Its Prediction and Verification

Eugene E. Covert, C. R. James, W. M. Kimzey, G. K. Richey,  
and E. C. Rooney, editors

Gives an authoritative, detailed review of the state-of-the-art of prediction and verification of the thrust and drag of aircraft in flight. It treats determination of the difference between installed thrust and drag of an aircraft and how it is complicated by interaction between inlet airflow and flow over the boattail and other aerodynamic surfaces. Following a brief historical introduction, chapters explore the need for a bookkeeping system, describe such a system, and demonstrate how aerodynamic interference can be explained. Subsequent chapters illustrate calculations of thrust, external drag, and throttle-induced drag, and estimation of error and its propagation. A commanding overview of a central problem in modern aircraft design.

**TO ORDER:** Write AIAA Order Department,  
370 L'Enfant Promenade, S.W., Washington, DC 20024  
Please include postage and handling fee of \$4.50 with all  
orders. California and D.C. residents must add 6% sales  
tax. All orders under \$50.00 must be prepaid. All foreign  
orders must be prepaid.

**1985 346 pp., illus. Hardback**  
**ISBN 0-930403-00-2**  
**AIAA Members \$49.95**  
**Nonmembers \$69.95**  
**Order Number V-98**